International Journal of Applied Pharmaceutics

ISSN- 0975-7058 Vol 17, Issue 1, 2025

Original Article

EXPLORING JACKFRUIT FLOUR POLYPHENOLS AS PROMISING SGLT-2 INHIBITORS FOR HYPERGLYCEMIA MANAGEMENT

SHASHANK M. PATIL[1], MANU G.[2], RAMYA C. M.[3], RAJASHEKHARA S.[4], SUDHANVA M. DESAI[5], SARAVANAN PARAMESWARAN[1], RAMITH RAMU[1]*

[1]Department of Biotechnology and Bioinformatics, JSS Academy of Higher Education and Research, Mysore–570015, Karnataka, India. [2]Department of Pharmacology, JSS Medical College, JSS Academy of Higher Education and Research, Mysore-570015, Karnataka, India. [3]Department of Physiology, JSS Medical College, JSS Academy of Higher Education and Research, Mysore-570015, Karnataka, India. [4]Department of Chemical Engineering, Siddaganga Institute of Technology, BH Road, Tumakuru-572103, Karnataka, India. [5]Department of Chemical Engineering, Dayananda Sagar College of Engineering, Bengaluru–560078, Karnataka, India

*Corresponding author: Ramith Ramu; *Email: ramith.gowda@gmail.com

Received: 04 Sep 2024, Revised and Accepted: 12 Nov 2024

ABSTRACT

Objective: This study explored the potential of dietary polyphenols from whole green jackfruit flour as natural Sodium-Glucose Co-Transporter-2 (SGLT-2) inhibitors for managing hyperglycemia in diabetes mellitus.

Methods: Advanced bio-computational techniques, including molecular docking, Molecular Dynamics (MD) simulations, and binding free energy calculations, were employed to identify and assess polyphenols from jackfruit flour. Caffeic and syringic acids were highlighted for their strong binding affinities to the SGLT-2 receptor. Additionally, a ligand-based pharmacophore model was developed using caffeic acid as a reference to screen for new lead compounds in commercial and natural product databases.

Results: The study found that caffeic acid and syringic acid exhibited stronger binding affinities and more stable interaction profiles with the SGLT-2 receptor than the standard drug empagliflozin. MD simulations demonstrated that these compounds provided greater stability in the binding site, indicating their potential efficacy as SGLT-2 inhibitors. The pharmacophore screening further supported these findings, identifying both compounds as promising lead candidates.

Among the 14 dietary polyphenols obtained from High-Performance Liquid Chromatography (HPLC), a molecular docking study suggested that caffeic acid (binding affinity:-9.0 kcal/mol) and syringic acid (binding affinity:-9.1 kcal/mol) exhibited stronger binding affinities and more stable interaction profiles with the SGLT-2 receptor compared to the standard drug empagliflozin (binding affinity:-10.4 kcal/mol). Further, molecular dynamics simulations demonstrated that these compounds provided greater stability in the binding site, indicating their potential efficacy as SGLT-2 inhibitors through Root mean Square Deviation (RMSD), Root mean Square Fluctuation (RMSF), Radius of Gyration (Rg), Solvent Accessible Surface Area (SASA), and ligand hydrogen bonds. The pharmacophore screening further supported these findings, identifying both compounds as promising lead candidates.

Conclusion: This study is the first to identify caffeic acid and syringic acid from whole green jackfruit flour as effective SGLT-2 inhibitors. These natural compounds show significant potential as novel agents for managing hyperglycemia and diabetes mellitus. The findings support further exploration of plant-derived therapies in diabetes treatment.

Keywords: SGLT-2 inhibitors, Caffeic acid, Syringic acid, Empagliflozin, Molecular docking, Molecular dynamics simulation, Binding free energy calculations

DOI: https://dx.doi.org/10.22159/ijap.2025v17i1.52573 Journal homepage: https://innovareacademics.in/journals/index.php/ijap

INTRODUCTION

Type-2 Diabetes Mellitus (T2DM) is a global chronic condition characterized by a range of metabolic disorders, including obesity, hypertension, heart failure, dyslipidemia, hyperuricemia, and renal failure. Additionally, individuals with T2DM are susceptible to complications such as diabetic neuropathy and retinopathy, which impact the nervous system and vision, respectively [1]. T2DM is also related to pulmonary diseases [2, 3]. Although various oral and intravenous glucose-lowering medications are widely used, the risk of cardiorenal complications in diabetic patients remains a significant concern [4].

Recent research has focused on identifying new molecular targets to mitigate the effects of diabetes mellitus. In this regard, Sodium-Glucose Co-Transporter (SGLT) proteins play a vital role in glucose reabsorption in the body. Sodium-glucose Co-Transporter-1 (SGLT-1), which has high affinity but low capacity, is mainly found in the kidneys' proximal tubules and the small intestine [5]. However, Sodium-Glucose Co-Transporter-2 (SGLT-2) proteins, responsible for over 90% of filtered glucose reabsorption, are considered prime targets for diabetes treatment. The standard renal glucose reabsorption threshold is around 180 mg/dl, but in T2DM patients, this threshold may increase due to SGLT-2 overexpression, exacerbating hyperglycemia. Selective SGLT-2 inhibitors can lower this threshold to between 40 and 120 mg/dl. SGLT-2 proteins are primarily located in the proximal convoluted tubules of the kidneys and are absent in the rare condition known as Familial Renal Glucosuria (FRG) [6, 7].

As the inhibition of SGLT-2 proves to be a proficient target for antidiabetic studies, several SGLT-2 inhibitor drugs have been proposed to date. SGLT-2 inhibitors allow glucose excretion in urine, preventing glucose reabsorption by inhibiting SGLT-2 in the Proximal Convoluted Tubule (PCT) [8]—elimination of glucose from the body, results in decreased plasma levels, thereby improving all glycemic markers. In 1835, the then-French chemists discovered phloridzin, a natural compound derived from the root bark of apple trees, initially used to treat malaria. Bioactive compounds isolated from banana flower and pseudostem extracts are proven to be cytoprotective, Deoxyribonucleic Acid (DNA) protective, antimicrobial, and thrombolytic [9, 10]. Today, drugs like empagliflozin, canagliflozin, and dapagliflozin, which target SGLT-2 inhibition, have received approval from the Food and Drug Administration (FDA) for managing diabetes mellitus. However, these SGLT-2 inhibitors come with several side effects. One of the most common issues is an increased risk of vaginal infections, with a fourfold rise observed during clinical trials. Patients experiencing severe hyperglycemia and glycosuria are more susceptible to

mycotic infections due to the presence of glucose in the urine. Additionally, SGLT-2 inhibition can lead to osmotic diuresis, causing volume depletion (hypovolemia), which manifests as frequent urination, excessive thirst, and orthostatic hypotension. Although urinary tract infections, genital mycotic infections, and osmotic diuresis-related symptoms were more frequently reported in clinical studies, they were generally mild to moderate severity [11, 12].

The phytochemical intervention of diabetes mellitus has been the centre of attraction in the current scenario. Several plants have been proven with their antidiabetic effects in various dimensions including *in vitro*, *in vivo*, and *in silico* approaches. Jackfruit (*Artocarpus heterophyllus*), also referred to as the jack tree, is a species of tree belonging to the mulberry, breadfruit, and fig families (*Moraceae*), and it is native to Southeast Asia, originating from India [13, 14]. Asthma, wounds, dermatosis, anemia, and diarrhea have all been treated using leaves and roots in the past. The phytochemical and pharmacological characteristics of the pulp of jackfruit, leaf, bark, and root have been studied [15]. By decreasing the generation of Prostaglandin E2 (PGE2) and Nitric Oxide (NO), the pulp extract of jackfruit has been shown to exhibit anti-inflammatory characteristics. Jackfruit leaf extracts, on the other hand, have antioxidant qualities and can help to lower hyperglycemia and hyperlipidemia [16].

However, the antidiabetic effect of jackfruit has yet to be explored in different aspects. Since the computational tools offer a great opportunity to virtually examine and validate the pharmacological experiments, we aim to find a suitable inhibitor for SGLT-2 using the same. Through this study, we aim to virtually screen the whole jackfruit compounds obtained from High-Performance Liquid Chromatography (HPLC) analysis as the SGLT-2 inhibitors. With the outcomes from computational studies, this study becomes a pavement for the discovery of jackfruit phytochemicals as site-specific inhibitors of SGLT-2, which can be adopted for biological evaluation in the near future.

MATERIALS AND METHODS

Molecular docking simulations

The X-ray crystallographic structure of the human Sodium-Glucose Co-Transporter-2– Membrane-Associated Protein 17 (SGLT-2-MAP17) complex bound to empagliflozin (PDB ID: 7VSI) was retrieved, along with the associated ligand structures, from the Research Collaboratory for Structural Bioinformatics Protein Data Bank (RCSB PDB) and PubChem databases, building on previous work by the researchers [17]. Empagliflozin served as the control in this study. To prepare the protein and ligand structures for molecular docking simulations, AutoDock Tools 1.5.6 was employed, following methodologies outlined in earlier studies by the authors [18-20]. A thorough literature review was undertaken to accurately predict the binding sites of the target protein [21]. The protein's binding pocket was defined within a grid box measuring 16.84 Å × 16.84 Å × 16.84 Å, with coordinates set at x = 38.30 Å, y = 50.24 Å, and z = 46.38 Å using AutoDock Tools 1.5.6.

The phytocompounds were subjected to virtual screening using AutoDockVina 1.1.2, a command-line software tool. The Broyden-Fletcher-Goldfarb-Shanno (BFGS) algorithm was employed to manipulate and correctly position the ligands within the target site and to evaluate the scoring function for each ligand's conformation [22, 23]. Due to the high number of torsional angles generated during ligand formation, the ligands were treated as flexible, while the protein remained rigid throughout the docking process. However, 10 degrees of freedom were allowed for the ligands. Among the ten binding poses produced, the first one, showing a Root-Mean-Square Deviation (RMSD) of zero, was deemed the most precise and demonstrated the highest binding affinity, indicating a more effective binding interaction. The molecular docking simulations were visualized using Biovia Discovery Studio Visualizer 2021, an open-source graphical user interface software. The interaction strength of the ligands was assessed based on the total number of bonds, specific hydrogen bonds, and binding affinity [24, 25].

Molecular dynamics simulations

To conduct the Molecular Dynamics (MD) simulation, SGLT-2 protein complexes bound to empagliflozin, syringic acid, and caffeic acid were chosen based on their strongest negative binding affinities. The simulations were performed using GROningen MAchine for Chemical Simulations 2018.1 (GROMACS 2018.1), a comprehensive biomolecular software package as cited in the study by Patil *et al.* (2021) [26]. GROMACS 2018.1 is a robust software suite designed for molecular dynamics, facilitating the simulation of Newtonian equations of motion for systems that range from hundreds to millions of particles. This software is particularly adept at handling biological compounds like nucleic acids, proteins, and lipids, and is especially efficient at calculating nonbonded interactions, which frequently occur and are critical in simulations [27, 28]. The MD simulations included not only the protein complexes with empagliflozin, syringic acid, and caffeic acid but also a simulation of the protein's bare backbone. Four separate simulations were conducted, each lasting 100 nanoseconds at a controlled temperature of 310K and a pressure of 1 bar. The resulting data, including RMSD, Root-Mean-Square Fluctuation (RMSF), Radius of Gyration (Rg), Solvent-Accessible Surface Area (SASA), and ligand hydrogen bond trajectories, were analyzed using GRaphing, Advanced Computation and Exploration of data (GRACE), a specialized graphical user interface for visualizing MD simulation results [29, 30].

Free energy landscape (FEL) analysis

Besides MD simulation, Principal Component Analysis (PCA) was conducted to assess the conformational changes during the protein-ligand complex simulation, following the methodology outlined by Patil *et al.* (2023) [31]. PCA serves as a powerful tool for identifying motion directions and statistically characterizing collective movements. The g_covar and g_anaeig utilities were employed to derive the two primary components – Primary Component 1 (PC1) and Primary Component 2 (PC2) by diagonalizing the matrix, using the essential dynamics protocol to protect these components. Moreover, the Gibbs FEL was constructed using PC1 and PC2 as reaction coordinates, offering valuable insights into the protein's conformational shifts and the dynamic behavior of the ligands.

Binding free energy (BFE) calculations

Following MD simulations, the binding free energy was assessed for the target proteins employing the Molecular Mechanics/Poisson-Boltzmann Surface Area (MM-PBSA) method. This approach integrates MD simulations with thermodynamic principles to evaluate the ligand's binding interaction with the protein. For each ligand-protein complex, the g_mmpbsa tool was employed along with the MmPbSaStat. py script, processing trajectory data generated by GROMACS 2018.1 as input. The g_mmpbsa tool calculates binding free energy by considering three components: molecular mechanical energy, polar solvation energy, and apolar solvation energy. The MD trajectories from the final 50 ns of the simulation were used to calculate free energy (ΔG), within a frame interval of 1000. The assessment of ΔG involves the combination of Molecular Mechanical Energy (MME) with polar and apolar solvation energies. The equations used for the binding free energy calculation are detailed in the following [32, 33].

$$\Delta G_{(Binding)} = G_{(Complex)} - [G_{(Protein)} + G_{(Ligand)}] \text{ -------- (I)}$$

$$\Delta G = \Delta E_{(MM)} + \Delta G_{(Solvation)} - T\Delta S = \Delta E_{(Bonded+non\text{-}bonded)} + \Delta G_{(Polar+non\text{-}polar)} - T\Delta S \text{ ------- (II)}$$

$G_{Binding}$: refers to the binding free energy, $G_{Complex}$: Represents the overall free energy of the protein-ligand complex, $G_{Protein,}$ and G_{Ligand}: Denote the total free energies of the isolated protein and ligand within the solvent, respectively, ΔG: The standard free energy change, ΔE_{MM}: The average molecular mechanics potential energy in a vacuum, $G_{Solvation}$: The energy associated with solvation, ΔE: Encompasses the total energy from both bonded and non-bonded interactions, ΔS. The entropy change in the system due to ligand binding, T: Temperature measured in Kelvin [34, 35].

Pharmacophore-based virtual screening (PBVS)

Pharmacophoric features were identified by analyzing the binding poses of the screened hits using a ligand-based 3D pharmacophore. The pharmacophore model was constructed with the help of the

Pharma Gist web server [32]. The selection of the appropriate pharmacophore model was guided by the critical intermolecular interactions between the screened hits and the SGLT-2 protein, using caffeic acid as the reference. This chosen pharmacophore model was then employed for virtual screening against the ZINC natural product database via ZINCPharmer, aiming to identify new inhibitors for human SGLT-2 [33]. The molecules identified from the ZINC purchasable compounds and natural product database were further subjected to Absorption, Distribution, Metabolism, Excretion, and Toxicity (ADMET) analysis using the Swiss ADME tool in Simplified Molecular Input Line Entry System (SMILES) format.

RESULTS AND DISCUSSION

Molecular docking simulation

Molecular docking analyses of phytocompounds identified via Reverse Phase High-Performance Liquid Chromatography (RP-HPLC) reveal that these phenolic compounds successfully bind to the active site of the human SGLT-2 protein, occupying the same position as the co-crystallized ligand 7R3703 in the SGLT-2 protein structure (PDB ID: 7VSI). Among the compounds examined for their affinity for binding and interaction, caffeic acid (-9.0 kcal/mol) and syringic acid (-9.1 kcal/mol) (fig. 1) demonstrated superior binding affinities, closely matching those of the control drug empagliflozin, which had a binding affinity of-10.4 kcal/mol. The results of the virtual screening are provided in (table 1). Given their promising binding affinities and significant intermolecular relations with human SGLT-2, the phenolic substances of syringic acid and caffeic acid were selected for further study. Although other compounds also exhibited a good tendency for binding, their physicochemical properties were not suitable for use as lead molecules. In particular, kaempferol and quercetin were excluded from further analysis due to their known adverse metabolic effects [36].

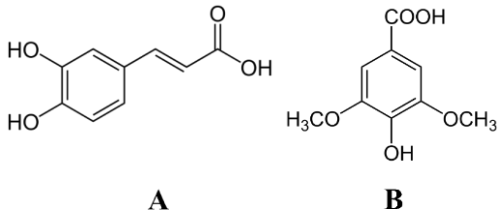

Fig. 1: Structures of key phenolic compounds A) caffeic acid and B) syringic acid from our earlier work [14]

Table 1: Overview of inter-molecular interaction data of ethanol extract of Jackfruit flour (EJF) phenolic compounds against human SGLT-2

S. No.	Name of the compound	Binding affinity (kcal/mol)	Total no. of intermolecular bonds	Total no. of hydrogen bonds
1	Ascorbic acid	-5.4	7	3
2	Gallic acid	-6.2	8	4
3	Catechin	-8.9	7	5
4	Rutin	-6.8	6	4
5	Methyl gallate	-6.4	5	2
6	Caffeic acid*	-9.0	6	5
7	Syringic acid*	-9.1	9	5
8	p-Coumaric acid	-6.6	7	3
9	Sinapic acid	-6.6	7	4
10	Ferulic acid	-6.9	8	4
11	Myricetin	-7.2	9	3
12	Apigenin	-7.8	6	3
13	Kaempferol	-9.2	7	4
14	Quercetin	-9.0	6	3
15	Empagliflozin*	-10.4	8	5

*The molecules investigated in the current study that might serve as lead molecules for further investigation on the inhibition of human SGLT-2

The active site/inhibitor binding site of SGLT-2 (PDB ID: 7VSI) is distributed between the helices M1b, M1a, M2, M6b, M7, and M10. The inhibitor binding site, located between these helices, is occupied by the co-crystallized ligand 7R3703. In the course of our research, it was discovered that every molecule occupied the same site of binding as 7R3703 (fig. 2). Binding interactions of caffeic acid, syringic acid, and empagliflozin followed the previously reported studies by Niu *et al.*, [37], where the compound LX2761 was found to be docked right at the inhibitory site of binding of the protein-SGLT-2 (PDB ID: 7VSI). Both caffeic and syringic acids were found to have the same binding interactions as reported by the study. It was also reported to correlate with a docking study by Kuswandi *et al.* (2022) [38], who reported *Garcinia atroviridis*-derived phytocompounds as the potential inhibitors of human SGLT-2 protein (PDB ID: 7VSI). With myricetin from *G. atroviridis* reported as the potential inhibitor of human SGLT-2 having binding interactions in the same vicinity, both caffeic acid and syringic acid can also be used as effective inhibitors of the same. However, within the inhibitory site, both studies have not reported to have found their compounds stable. Therefore, the stability of the reported compounds needs to be examined with molecular dynamics simulations for reliability to proceed with further investigations.

Important residues of the inhibitor binding site, such as Trp291, Lys321, Phe98, Glu99, Leu283, and Tyr290, which are situated between the helices M1, M2, M6, M7, and M10, have been attached to both caffeic acid and syringic acid. These interactions were also observed in previous studies that used the same PDB (7VSI) [38, 39]. Detailed interactions of caffeic acid and syringic acid, along with the positive control molecule, empagliflozin, with the human SGLT-2 residues are tabulated in table 2. Also, a visualization of the bound sites and their interaction with the compounds has been portrayed in fig. 3.

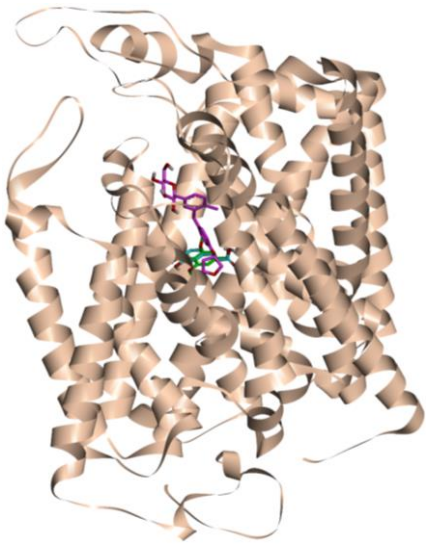

Fig. 2: Site of Inhibitor-binding of the human protein SGLT-2 with bound compounds. Cyan: caffeic acid, green: syringic acid, and pink: empagliflozin

Table 2: Binding interactions of caffeic acid, syringic acid, and empagliflozin with human SGLT-2 protein with distance in angstroms (Å)

Compounds	Hydrogen bonds	Hydrophobic interactions		
		(Π-Π) interaction	(Alkyl) interaction	(Π-alkyl) interaction
Caffeic acid	Trp291 (3.30), Lys321 (3.28), Ser460 (3.10), Phe98 (2.13), Gln457 (3.62)	Tyr290 (4.18)	-	
Syringic acid	Trp 291 (3.32), Lys231 (3.34), Gln457 (2.73), Phe98 (2.40), Glu99 (2.60)	Tyr290 (3.75),	Leu283 (5.01), Val286 (3.99), His80 (4.73)	
Empagliflozin	Thr87 (3.12), Ser287 (3.14), Trp291 (3.38), Thr87 (2.25), Gln457 (3.44)	Tyr290 (4.80)	-	Tyr290 (4.58), Leu84 (5.37)

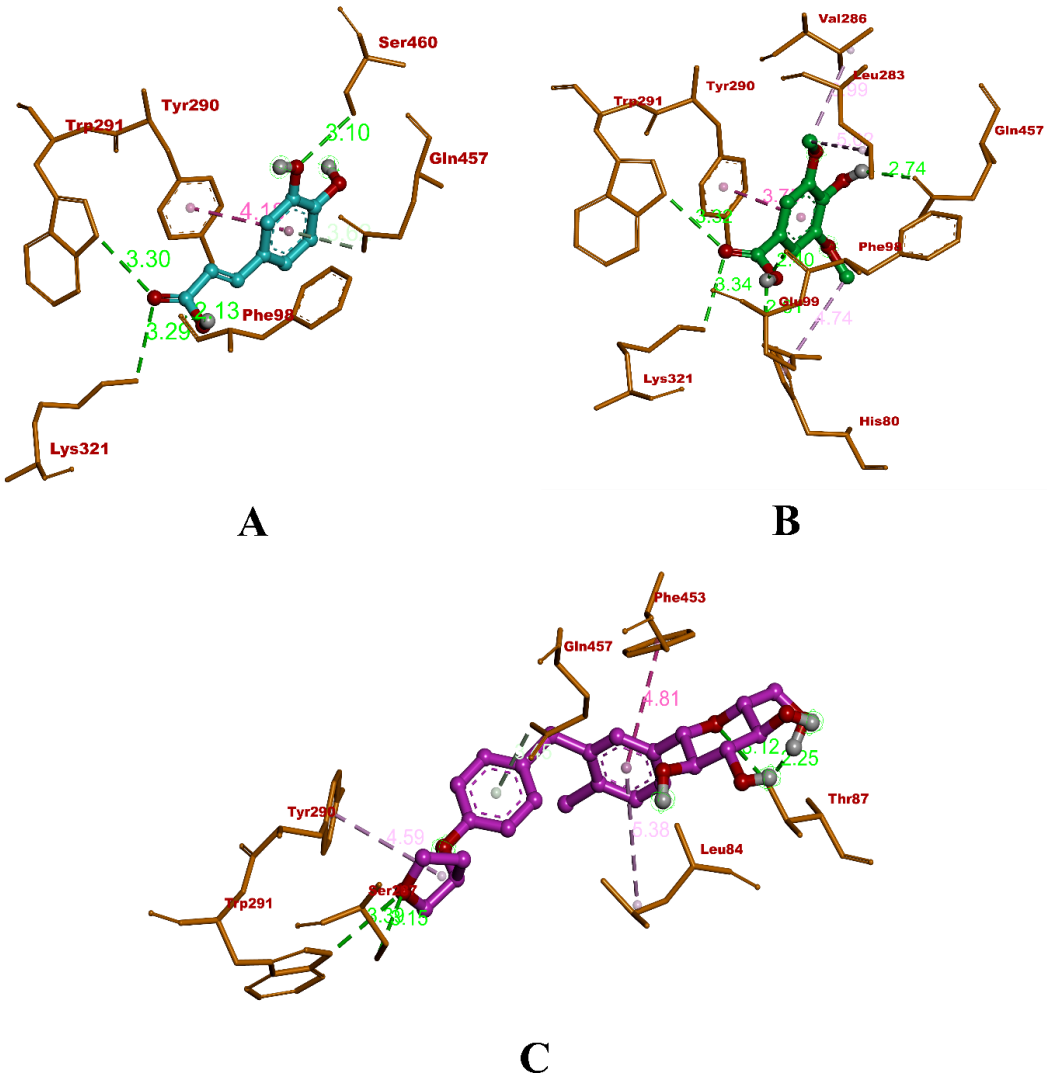

Fig. 3: Visualization of binding interactions of the compounds with SGLT-2 protein. Cyan: caffeic acid, green: syringic acid, and pink: empagliflozin

MD simulation

MD simulation offers deep structural and energetic insights into protein-ligand interactions. To evaluate the kinetics, elasticity, and durability of protein-ligand complexes, we examined parameters such as RMSF, RMSD, Rg, and SASA along with ligand-hydrogen bonds over a 100 ns trajectory. The RMSD metric, which reflects the stable conformation of the complex during the simulation, was a focal point of our analysis. We specifically monitored the RMSD of the optimized protein along with its atoms of the backbone. Throughout the RMSD calculations, the protein backbone atoms along with the complexes demonstrated an identical stability pattern. None of the molecules left the protein's active site throughout the simulation. The protein backbone atoms stabilized after 30 ns, while the complexes of caffeic acid and syringic acid achieved stability after 10 ns and 20 ns, respectively. In contrast, the empagliflozin-protein complex stabilized only after 50 ns. The RMSD values for the caffeic acid and syringic acid complexes closely matched those atoms of the backbone of the protein.

Besides RMSD, RMSF is pivotal for predicting conformational stability because residual fluctuations indicate the binding pose and interaction of ligands [24]. The protein backbone atoms show fluctuation at N-and C-terminals. High fluctuations were observed in the loop region residues (150-200). Both the caffeic acid and syringic acid complexes evince lower deviations in the beginning (at N-terminals) and throughout the simulation compared to empagliflozin. Further, Rg has provided insights into the folding and unfolding of proteins onto binding ligands, along with the compactness of the binding [25]. A protein with a stable fold will

likely maintain a relatively stable Rg during simulation. The analysis of the Rg plot manifests protein, empagliflozin, caffeic acid, and syringic acid complexes having similar compactness. These results indicate that the binding of each compound significantly stabilized the structure of the protein.

Computing SASA helps in examining modifications in the solvent reactivity of proteins [26]. This value could be used to study interactions between and within proteins, ligands, and solvents. All the SASA plots show decreasing values since the SASA is occupied by the ligands. Numerically similar values also indicate that the ligands' binding is in a similar pattern. Bonds between ligands and hydrogens are crucial for determining the structure re-agreement in dynamic trajectory analysis [27]. During MD simulation, phenolic compounds from the caffeic and syringic acid present the highest nos. of H bonds, compared to empagliflozin. Based on the results of outcomes of the MD simulation, caffeic acid, along with syringic acid, may potentially stimulate biological activity in the binding site of the inhibitor by connecting to the key residues. The values of MD trajectories have been summarized in table 4 and fig. 4 represents the different trajectories of molecular dynamics simulation. The overall stability of both caffeic acid and syringic acid reported in our study is by Arif *et al.* (2021) [40], where a polypeptide from *Momordica charantia* was docked and simulated with SGLT-2 protein.

Table 4: Value of MD trajectories obtained from GROMACS 18.1 for different protein-ligand complexes

MD trajectories	Apo-protein	Caffeic acid-SGLT-2	Syringic acid-SGLT-2	Empagliflozin-SGLT-2
RMSD in (nm)	0.35-0.40	0.35-0.40	0.30-0.35	0.30-0.35
Maximum RMSF (nm);	(0.55-0.60)	(0.45-0.50)	(0.45-0.50)	(0.50-0.55)
Rg (nm)	0.20-0.25	0.20-0.25	0.20-0.25	0.20-0.25
SASA (nm^2)	180-185	175-180	175-180	180-185
Ligand H-bonds	not applicable	3	6	4

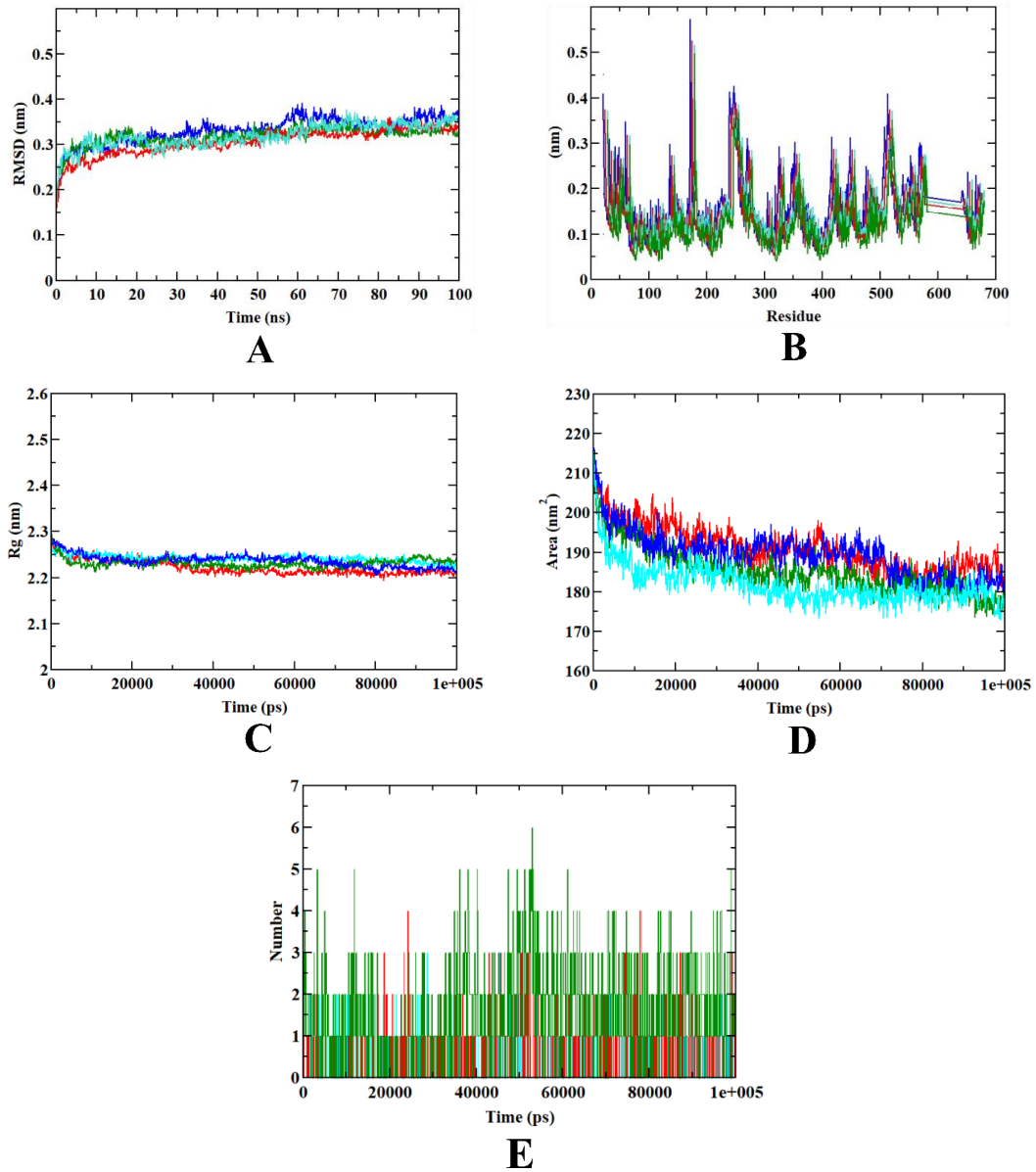

Fig. 4: Display illustrating MD trajectories for several protein-ligand complexes acquired from GROMACS 18.1. Protein-caffeic acid complex: cyan, protein-syringic acid complex: green, protein-empagliflozin complex: red, and apo-protein: blue

FEL analysis

The FEL of six systems were analyzed based on the top two principal components, PC1 and PC2, to assess the impact of drug binding on conformational shifts. Lower Gibbs free energy indicates effective ligand binding, stable complex formation, and favorable conformational changes (Pandey *et al.*, 2021) [41]. The SGLT-2 protein which is bound to both caffeic acid (0.0-8.98 kJ/mol) and syringic acid (0.0-8.3 kJ/mol) exhibited lower free energy levels. In contrast, the protein-empagliflozin complex (0.0–9.08 kJ/mol) had higher Gibbs free energy values. As opposed to the unbound protein structure (0.0-9.88 kJ/mol), the complexes with caffeic acid and syringic acid did not show a significant increase in Gibbs free energy. Elevated Gibbs free energy typically suggests less favorable conformational changes and reduced stability in the protein structure. Our FEL analysis results are consistent with a previous study by Bisha *et al.* (2014) [42], which explored the binding of a Na+ion within the inhibitor binding site of SGLT-2. The Gibbs free energy in this study ranges between 0.0 to-9.0 kJ/mol, which is the same in our study. Since there is a decrease in the Gibbs free energy in both caffeic acid and syringic acid-bound protein complexes, the SGLT-2 protein conformation changes are energetically favorable [29]. Fig. 5 depicts the FEL plots of experimental molecules bound with the target protein as well as the free proteins.

Table 5: BFE estimations of different protein-ligand binding complexes

Forms of BFEs	Caffeic acid-SGLT-2 complex (kJ/mol)	Syringic acid-SGLT-2 complex (kJ/mol)	Empagliflozin-SGLT-2 complex (kJ/mol)
Van der Waal energy	-153.748±12.328	-304.715±11.985	-145.927±12.231
Electrostatic energy	-4.685±7.026	-5.767±2.797	-5.234±1.891
Polar solvation energy	61.922±9.129	94.404±11.816	87.156±10.241
SASA energy	-11.092±7.144	-21.827±0.860	-20.457±2.201
Binding energy	-107.603±12.170	-237.905±15.905	-295.981±10.918

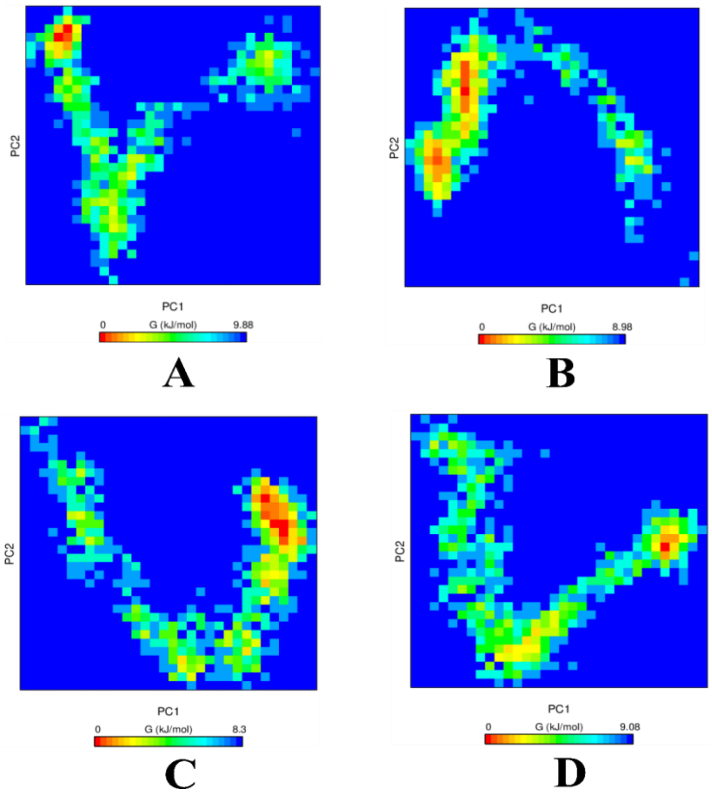

Fig. 5: The Gibbs FEL of various SGLT-2 protein-ligand complexes were analyzed using PCA. The landscape includes A) the SGLT-2 unbound protein or apo-protein structure, B) the SGLT-2 protein complexed with caffeic acid, C) the SGLT-2 protein with syringic acid, and D) the SGLT-2 protein bound to empagliflozin. The colored bar illustrates the Gibbs free energy values in kJ/mol

BFE calculations

The most significant indicator of therapeutic drug potency for drug design based on structure is the single most important indicator of drug potency is the *in silico* protein-ligand binding affinity prediction. For accurate predictions in the context of drug development programs, BFE simulations rely on statistical mechanics and physics-based molecular simulations [21, 22]. In this calculation, various factors were considered, including Van der Waals forces, electrostatic interactions, SASA, polar solvation, and binding energy [26]. The analysis reveals that Van der Waals energy primarily drives the formation of all protein-ligand complexes. The results indicate that complexes involving protein with phenolic acids, such as caffeic acid and syringic acid, exhibit greater stability compared to the protein-empagliflozin complex. Although all complexes are energetically favorable, the protein-phenolic acid complexes are notably more stable and reliable. Table 5 provides an overview of the calculations made for the BFE of protein-ligand complexes.

PBVS

Though the PharmaGist webserver provided several pharmacophore models, the appropriate pharmacophore model was selected based on the key intermolecular interactions between the screened hits and human SGLT-2 with caffeic acid as a reference molecule to facilitate the screening of lead molecules, which was presented in fig. 6. The pharmacophoric feature, Hydrogen bond acceptor was chosen to facilitate interactions with

Lys321, Ser287, and Thr153 of SGLT-2 protein while Hydrogen bond acceptor facilitated the interaction with Thr153 of SGLT-2 protein. The hydrophobic pharmacophoric feature enables the aromatic ring from the virtually screened hits to form Pi-Pi stacked hydrophobic interaction with Tyr290 of human SGLT-2.

The PBVS yielded 7826 and 607 from ZINC purchasable compounds and natural products database, respectively. The RMSD measure from ZINCPharmer is applied to filter the hits with 0.25Å cutoff yield of 675 and 27 molecules, respectively, and the top three hits based on RMSD are presented in table 6.

Table 6: The top 10 screened ZINC purchasable compounds and natural products database from PBVS with caffeic acid as reference molecule

ZINC purchasable compounds database from PBVS			ZINC natural products database from PBVS		
ZINC Id	**2D structure**	**RMSD#**	**ZINC Id**	**2D structure**	**RMSD#**
ZINC02015035*	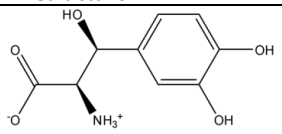	0.130089	ZINC91968790	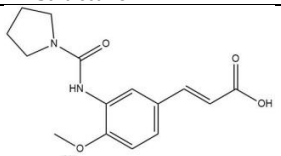	0.144708
ZINC01564653*	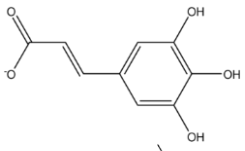	0.145571	ZINC77285163	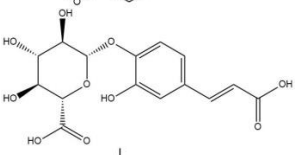	0.14493
ZINC00895821*	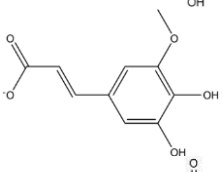	0.145639	ZINC91993129	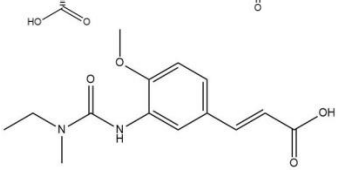	0.145506
ZINC01592824	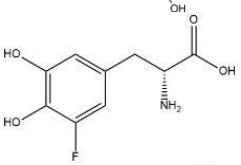	0.148831	ZINC91961112	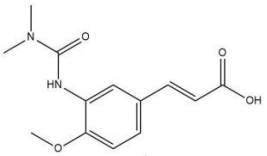	0.145507
ZINC02005215	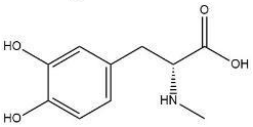	0.149301	ZINC95038058	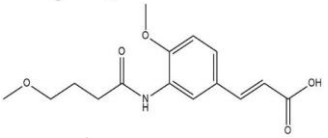	0.145619
ZINC01482068	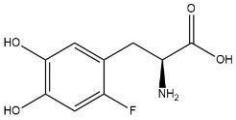	0.177355	ZINC91962572	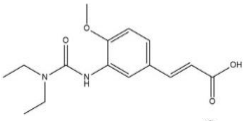	0.14563
ZINC13458828	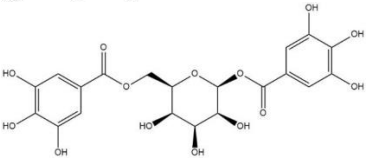	0.17978	ZINC91365352	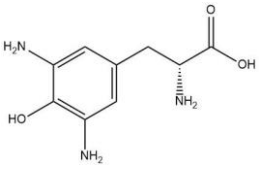	0.150721
ZINC15043216	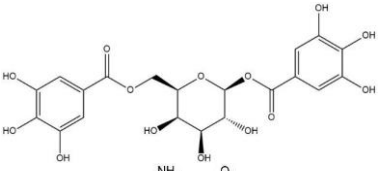	0.183071	ZINC06170676	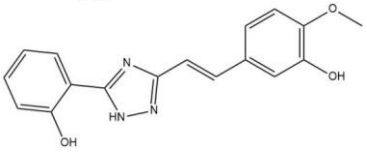	0.15138
ZINC12649959	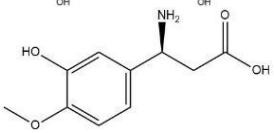	0.190866	ZINC01585592	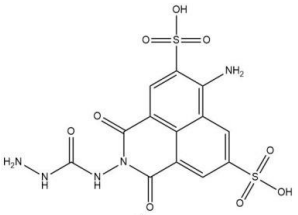	0.155522
ZINC00388044	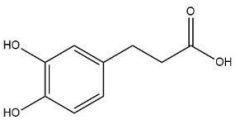	0.191226	ZINC94610848	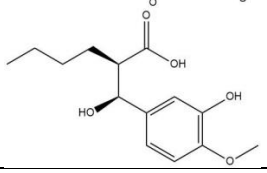	0.155691

#-ZINC Pharmer RMSD

The top ten hits from ZINC purchasable compounds and natural compounds database were subjected to ADMET analysis. It was discovered that syringic acid and caffeic acid both had a bioavailability score of 0.55 and did not violate Lipinski's rule of five. The same was shown in our earlier research, where the inhibition of α-glucosidase, α-amylase, and aldose reductase *in silico* and *in vitro* was assessed for caffeic acid and syringic acid [15]. Regarding ZINC purchasable compounds, no compound was discovered to violate Lipinski's rule of five. Compounds ZINC13458828 (4.75), ZINC15043216 (4.75), and ZINC01564653 (1.92) were the top 3 molecules with the best bioavailability score. The ADME evaluation has been presented in detail in table 7.

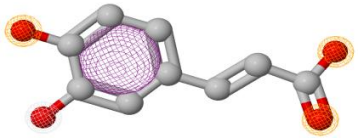

Fig. 6: The chosen pharmacophore model with highlighted pharmacophoric features for the screening of lead molecules against human SGLT-2 with caffeic acid as a reference molecule. Three hydrogen bond acceptors, one hydrogen bond donor, and one hydrophobic feature are represented by orange, white, and magenta circles, respectively, in the pharmacophore model

Table 7: ADME properties of top 10 natural products and ZINC purchasable compounds

S. No.	Compound	MW	NRB	NHBA	NHDA	TPSA	LogP	CYP inhibition	BBB	Bioavailability
Top 10 virtually screened compounds from the PubChem database based on our earlier work										
1	Caffeic acid	180.16	2	4	3	77.76 Å²	0.93	No	No	0.56
2	Syringic acid	198.17	3	5	2	75.99 Å²	0.99	No	No	0.56
3	p-Coumaric acid	164.16	2	3	2	57.53 Å²	1.26	No	No	0.85
4	Sinapic acid	224.21	4	5	2	75.99 Å²	1.31	No	No	0.56
5	Ferulic acid	194.18	3	4	2	66.76 Å²	1.36	No	No	0.85
6	Myricetin	318.24	1	8	6	151.59 Å²	0.79	No	No	0.55
7	Apigenin	270.24	1	5	3	90.90 Å²	2.11	No	No	0.55
8	Kaempferol	286.24	1	6	4	111.13 Å²	1.58	No	No	0.55
9	Quercetin	302.24	1	7	5	131.36 Å²	1.23	No	No	0.55
10	Catechin	290.27	1	6	5	110.38 Å²	0.85	No	No	0.55
11	Empagliflozin	450.91	6	7	4	108.61 Å²	2.01	No	No	0.55
ZINC Purchasable Compounds and Natural Products Database from PBVS										
1	ZINC02015035	213.19	3	6	5	124.01 Å²	-1.58	No	No	0.55
2	ZINC01564653	196.16	2	5	4	97.99 Å²	0.60	No	No	1.92
3	ZINC00895821	210.18	3	5	3	86.99 Å²	1.01	No	No	0.56
4	ZINC01592824	215.18	3	6	4	103.78 Å²	-0.53	No	No	0.55
5	ZINC02005215	211.21	4	5	4	89.79 Å²	-0.49	No	No	0.55
6	ZINC01482068	215.18	3	6	4	103.78 Å²	-0.44	No	No	0.55
7	ZINC13458828	484.36	7	14	9	243.90 Å²	-1.00	No	No	4.75
8	ZINC15043216	484.36	7	14	9	243.90 Å²	-1.00	No	No	4.75
9	ZINC12649959	211.21	4	5	3	92.78 Å²	0.04	No	No	0.55
10	ZINC00388044	182.17	3	4	3	77.76 Å²	0.63	No	No	0.56
11	ZINC91968790	290.31	6	4	2	78.87 Å²	1.72	No	No	0.56
12	ZINC77285163	356.28	5	10	6	173.98 Å²	-1.16	No	No	0.11
13	ZINC91993129	278.30	7	4	2	78.87 Å²	1.61	No	No	0.56
14	ZINC91961112	264.28	6	4	2	78.87 Å²	1.29	No	No	0.56
15	ZINC95038058	293.32	9	5	2	84.86 Å²	1.73	No	No	0.56
16	ZINC91962572	292.33	8	4	2	78.87 Å²	2.02	No	No	0.56
17	ZINC91365352	211.22	3	4	5	135.59 Å²	-1.45	No	No	0.55
18	ZINC06170676	309.32	4	5	3	91.26 Å²	2.61	No	No	0.55
19	ZINC01585592	445.38	5	10	6	257.74 Å²	-2.24	No	No	0.11
20	ZINC94610848	268.31	7	5	3	86.99 Å²	1.94	No	No	0.56

Note: Molecular Weight (MW), Number of Rotatable Bonds (NRB), Number of Hydrogen Bonds Acceptor (NHBA), Number of Hydrogen Bonds Donor (NHDA), Topological Polar Surface Area (TPSA), The base-10 logarithm of the partition coefficient P (LogP), Cytochrome P (CYP), and Blood-Brain Barrier (BBB).

CONCLUSION

The SGLT-2 inhibitors are a promising family of medications that can effectively treat hyperglycemia and undoubtedly assist a huge number of diabetic people in a safe and tolerable manner. Their distinct mode of action, blood pressure management, and pleiotropic effects make them suitable as alternative strategies for people who are not well-controlled by conventional treatments. In this study, the potent phenolic compounds from whole green jackfruit flour were investigated as potential inhibitors against human SGLT-2 protein. Among the examined compounds, both caffeic acid and syringic acid showed higher binding efficiency through molecular docking, binding with key residues of human SGLT-2 that could induce inhibition of the protein activity. Additionally, these compounds also demonstrated favorable stability and binding affinity during MD simulations and BFE estimations, suggesting their potential to act similarly to the conventional SGLT-2 inhibitor empagliflozin. Moreover, pharmacophore modeling suggests that the caffeic acid can serve as a lead molecule with 5 features and subsequent virtual screening against ZINC purchasable compounds and natural products database yielded 675 and 27 molecules, respectively for further study. While pharmacological investigations are needed to confirm their biological efficacy, these findings suggest that both caffeic acid and syringic acid could show potential leads for developing SGLT-2 inhibitors for the treatment of hyperglycemia in diabetes mellitus.

ACKNOWLEDGMENT

The authors express their gratitude to the JSS Academy of Higher Education and Research in Mysore, Karnataka, India, for their generous support, encouragement, and provision of essential facilities.

FUNDING

This research received no external funding.

ABBREVIATIONS

Absorption, Distribution, Metabolism, Excretion, and Toxicity (ADMET), Binding Free Energy (BFE), Blood-Brain Barrier (BBB), Broyden-Fletcher-Goldfarb-Shanno (BFGS), Cytochrome P (CYP), Deoxyribonucleic acid (DNA), Ethanol Extract of Jackfruit Flour (EJF), Familial Renal Glucosuria (FRG), Food and Drug Administration (FDA), Free Energy Landscapes (FEL), High-Performance Liquid Chromatography (HPLC), GRaphing, Advanced Computation and Exploration of data (GRACE), GROningen MAchine for Chemical Simulations 2018.1 (GROMACS 2018.1), Molecular Dynamics (MD), Molecular Mechanical Energy (MME), Molecular Weight (MW), Nitric Oxide (NO), Number of Hydrogen Bonds Acceptor (NHBA), Number of Hydrogen Bonds Donor (NHDA), Number of Rotatable Bonds (NRB), Pharmacophore-Based Virtual Screening (PBVS), Primary Component 1 (PC1), Primary Component 2 (PC2), Principal Component Analysis (PCA), Prostaglandin E2 (PGE2), Proximal Convoluted Tubule (PCT), Radius of Gyration (Rg), Research Collaboratory for Structural Bioinformatics Protein Data Bank (RCSB PDB), Reverse Phase High-Performance Liquid Chromatography (RP-HPLC), Root mean Square Deviation (RMSD), Root mean Square Fluctuation (RMSF), Sodium-Glucose Co-Transporter (SGLT), Sodium-Glucose Co-Transporter-1 (SGLT-1), Sodium-Glucose Co-Transporter-2 (SGLT-2), Sodium-Glucose Co-Transporter-2– Membrane-Associated Protein 17 (SGLT-2-MAP17), Solvent Accessible Surface Area (SASA), Simplified Molecular Input Line Entry System (SMILES), The base-10 logarithm of the partition coefficient P (LogP), Topological Polar Surface Area (TPSA), Type 2 Diabetes Mellitus (T2DM)

AUTHOR CONTRIBUTIONS

The manuscript was planned and conceptualized by R. R. Data analysis and method development were conducted by S. M. P., M. G, and R. C. M. Supervision and editing were carried out by S. P., R. S., and S. M. D. All authors have reviewed and approved the final version of the manuscript.

CONFLICTS OF INTERESTS

All authors declare no conflict of interest.

REFERENCES

1. Patil SM, Shirahatti PS, Ramu R. Azadirachta indica A. juss (neem) against diabetes mellitus: a critical review on its phytochemistry pharmacology and toxicology. J Pharm Pharmacol. 2022 May 20;74(5):681-710. doi: 10.1093/jpp/rgab098, PMID 34562010.
2. Prashanth K, KS, Patil MS, Ramu R. A systematic review on enhanced transmission and effects of severe acute respiratory syndrome coronavirus 2: an Indian scenario. Asian J Pharm Clin Res. 2020 Nov 7;13(11):18-24. doi: 10.22159/ajpcr.2020.v13i11.39261.
3. VB CK, Patil SM, Shirahatti PS, SS, Ranganatha LV, MKJ, Ramu R. The current status and perspectives for the emerging pandemic: COVID-19. Int J Pharm Pharm Sci. 2020 Aug 1;12(8):1-10. doi: 10.22159/ijpps.2020v12i8.38206.
4. Simha NA, Patil SM, MK J, NC, Wong LS, Kijsomporn J. From sugar binders to diabetes fighters: the lectin saga of antihyperglycemic activity through systematic review and meta-analysis. Front Pharmacol. 2024 Sep 11;15:1382876. doi: 10.3389/fphar.2024.1382876, PMID 39323638.
5. Abdul Ghani MA, Norton L, DE Fronzo RA. Renal sodiumglucose cotransporter inhibition in the management of type 2 diabetes mellitus. Am J Physiol Renal Physiol. 2015;309(11):F889-900. doi: 10.1152/ajprenal.00267.2015, PMID 26354881.
6. Abdul Ghani MA, Norton L, Defronzo RA. Role of sodium-glucose cotransporter 2 (SGLT 2) inhibitors in the treatment of type 2 diabetes. Endocr Rev. 2011;32(4):515-31. doi: 10.1210/er.2010-0029, PMID 21606218.
7. Patil SM, MK J, Ramu R. Sestrin 2 as a new biomarker in obesity and diabetes mellitus: a new key player in the metabolic regulation. Int J Health Allied Sci. 2024;13(1):34.e41. doi: 10.55691/2278-344X.1090.
8. Fonseca Correa JI, Correa Rotter R. Sodium-glucose cotransporter 2 inhibitors mechanisms of action: a review. Front Med (Lausanne). 2021;8:777861. doi: 10.3389/fmed.2021.777861, PMID 34988095.
9. Ramu RA, Shirahatti PS, Zameer FA, Lakkapa DB, Nagendra M. Evaluation of Banana (Musa sp. var. Nanjangud Rasa bale) flower and pseudostem extracts on antimicrobial cytotoxicity and thrombolytic activities. Int J Pharm Pharm Sci. 2015;7(1):136-40.
10. Ramu R, Shirahatti PS, Bajpe SN, S VR, Nagendra Prasad MN. Impact of active compounds isolated from banana (Musa sp. var. nanjangud rasabale) flower and pseudostem towards cytoprotective and dna protection activities. Int J Pharm Pharm Sci. 2017;9(10). doi: 10.22159/ijpps.2017v9i10.20560.
11. Hsia DS, Grove O, Cefalu WT. An update on sodium-glucose co-transporter-2 inhibitors for the treatment of diabetes mellitus. Curr Opin Endocrinol Diabetes Obes. 2017;24(1):73-9. doi: 10.1097/MED.0000000000000311, PMID 27898586.
12. Ferrannini E. Sodium-glucose co-transporters and their inhibition: clinical physiology. Cell Metab. 2017;26(1):27-38. doi: 10.1016/j.cmet.2017.04.011, PMID 28506519.
13. Kalra S. Sodium-glucose co-transporter-2 (sglt2) inhibitors: a review of their basic and clinical pharmacology. Diabetes Ther. 2014;5(2):355-66. doi: 10.1007/s13300-014-0089-4, PMID 25424969.
14. Zhang L, TU ZC, Xie X, Wang H, Wang H, Wang ZX. Jackfruit (Artocarpus heterophyllus Lam.) peel: a better source of antioxidants and a-glucosidase inhibitors than pulp flake and seed and phytochemical profile by HPLC-QTOF-MS/MS. Food Chem. 2017;234:303-13. doi: 10.1016/j.foodchem.2017.05.003, PMID 28551240.
15. Maradesha T, Patil SM, Al-Mutairi KA, Ramu R, Madhunapantula SV, Alqadi T. Inhibitory effect of polyphenols from the whole green jackfruit flour against α-glucosidase α-amylase aldose reductase and glycation at multiple stages and their interaction: inhibition kinetics and molecular simulations. Molecules. 2022;27(6):1888. doi: 10.3390/molecules27061888, PMID 35335251.
16. Baliga MS, Shivashankara AR, Haniadka R, Dsouza J, Bhat HP. Phytochemistry nutritional and pharmacological properties of Artocarpus heterophyllus Lam (jackfruit): a review. Food Res Int. 2011;44(7):1800-11. doi: 10.1016/j.foodres.2011.02.035.
17. Simha N AN, Patil SM, Chagalamari A, Satish AM, Ramu R. Protocol to identify multiple protein targets and therapeutic compounds using an in silico polypharmacological approach. Star Protoc. 2023 Sep 15;4(3):102440. doi: 10.1016/j.xpro.2023.102440, PMID 37561634.
18. Maradesha T, Patil SM, Phanindra B, Achar RR, Silina E, Stupin V. Multiprotein inhibitory effect of dietary polyphenol Rutin from whole green jackfruit flour targeting different stages of diabetes mellitus: defining a bio-computational stratagem. Separations. 2022;9(9):262. doi: 10.3390/separations9090262.
19. Patil SM, Martiz RM, Ramu R, Shirahatti PS, Prakash A, Kumar BR. Evaluation of flavonoids from banana pseudostem and flower (quercetin and catechin) as potent inhibitors of α-glucosidase: an in silico perspective. J Biomol Struct Dyn. 2022;40(23):12491-505. doi: 10.1080/07391102.2021.1971561, PMID 34488558.
20. Martiz RM, Patil SM, Abdulaziz M, Babalghith A, Al-Areefi M, Al-Ghorbani M. Defining the role of isoeugenol from *Ocimum tenuiflorum* against diabetes mellitus linked alzheimers disease through network pharmacology and computational methods. Molecules. 2022;27(8):2398. doi: 10.3390/molecules27082398, PMID 35458596.
21. Patil SM, Martiz RM, Ramu R, Shirahatti PS, Prakash A, Chandra SJ. In silico identification of novel benzophenone coumarin derivatives as SARS-CoV-2 RNA-dependent RNA polymerase (RdRp) inhibitors. J Biomol Struct Dyn. 2022;40(23):13032-48. doi: 10.1080/07391102.2021.1978322, PMID 34632942.
22. Martiz RM, Patil SM, Ramu R, MK J, PA, Ranganatha LV. Discovery of novel benzophenone integrated derivatives as anti-Alzheimers agents targeting presenilin-1 and presenilin-2 inhibition: a computational approach. Plos One. 2022;17(4):e0265022. doi: 10.1371/journal.pone.0265022, PMID 35395008.
23. Kumar V, Shetty P, HS A, Chandra KS, Ramu R, Patil SM. Potential fluorinated anti-MRSA thiazolidinone derivatives with antibacterial antitubercular activity and molecular docking

studies. Chem Biodivers. 2022;19(2):e202100532. doi: 10.1002/cbdv.202100532, PMID 34929067.

24. Kumar V, Ramu R, Shirahatti PS, Kumari VC, Sushma P, Mandal SP. α-glucosidase; α-amylase inhibition; kinetics and docking studies of novel (2-chloro-6-(trifluoromethyl) benzyloxy) arylidene based rhodanine and rhodanine acetic acid derivatives. Chem Select. 2021;6(36):9637-44. doi: 10.1002/slct.202101954.
25. Sreepathi N, Kumari VB, Huligere SS, Al Odayni AB, Lasehinde V, Jayanthi MK. Screening for potential novel probiotic levilactobacillus brevis ramulab52 with antihyperglycemic property from fermented Carica papaya L. Front Microbiol. 2023 Jun 20;14:1168102. doi: 10.3389/fmicb.2023.1168102, PMID 37408641.
26. Patil SM, Maruthi KR, Bajpe SN, Vyshali VM, Sushmitha S, Akhila C. Comparative molecular docking and simulation analysis of molnupiravir and remdesivir with SARS-CoV-2 RNA dependent RNA polymerase (RdRp). Bioinformation. 2021;17(11):932-9. doi: 10.6026/97320630017932, PMID 35655903.
27. Ajala A, Eltayb WA, Abatyough TM, Ejeh S, El fadili M, Otaru HA. In silico screening and ADMET evaluation of therapeutic MAO-B inhibitors against parkinson disease. Intell Pharm. 2024 Aug 1;2(4):554-64. doi: 10.1016/j.ipha.2023.12.008.
28. Pradeep S, Patil SM, Dharmashekara C, Jain A, Ramu R, Shirahatti PS. Molecular insights into the in silico discovery of corilagin from Terminalia chebula as a potential dual inhibitor of SARS-CoV-2 structural proteins. J Biomol Struct Dyn. 2023 Dec;41(20):10869-84. doi: 10.1080/07391102.2022.2158943, PMID 36576118.
29. Huligere SS, Chandana Kumari VB, Alqadi T, Kumar S, Cull CA, Amachawadi RG. Isolation and characterization of lactic acid bacteria with potential probiotic activity and further investigation of their activity by α-amylase and α-glucosidase inhibitions of fermented batters. Front Microbiol. 2022;13:1042263. doi: 10.3389/fmicb.2022.1042263, PMID 36756202.
30. Nivetha N, Martiz RM, Patil SM, Ramu R, Sreenivasa S, Velmathi S. Benzodioxole grafted spirooxindole pyrrolidinyl derivatives: synthesis characterization molecular docking and anti-diabetic activity. RSC Adv. 2022;12(37):24192-207. doi: 10.1039/D2RA04452H, PMID 36128541.
31. Patil SM, Phanindra B, Shirahatti PS, Martiz RM, Sajal H, Babakr AT. Computational approaches to define poncirin from Magnolia champaka leaves as a novel multi-target inhibitor of SARS-CoV-2. J Biomol Struct Dyn. 2023;41(22):13078-97. doi: 10.1080/07391102.2023.2171137, PMID 36695109.
32. Gurupadaswamy HD, Ranganatha VL, Ramu R, Patil SM, Khanum SA. Competent synthesis of biarylanalogs via asymmetric suzuki miyaura cross-coupling for the development of anti-inflammatory and analgesic agents. J Iran Chem Soc. 2022;1:1-16.
33. Ganavi D, Ramu R, Kumar V, Patil SM, Martiz RM, Shirahatti PS. *In vitro* and in silico studies of fluorinated 2,3-disubstituted thiazolidinone pyrazoles as potential α-amylase inhibitors and antioxidant agents. Arch Pharm (Weinheim). 2022;355(3):e2100342. doi: 10.1002/ardp.202100342, PMID 34923670.
34. Patil SM, Al-Mutairi KA, Firdose N, Ramu R, Martiz RM, PA. Pharmacoinformatics-based screening discovers swertianolin from lavandula angustifolia as a novel neuromodulator targeting epilepsy, depression and anxiety. S Afr J Bot. 2022 Sep 1;149:712-30. doi: 10.1016/j.sajb.2022.06.054.
35. Sajal H, Patil SM, Raj R, Shbeer AM, Ageel M, Ramu R. Computer-aided screening of phytoconstituents from ocimum tenuiflorum against diabetes mellitus targeting DPP4 inhibition: a combination of molecular docking molecular dynamics and pharmacokinetics approaches. Molecules. 2022 Aug 12;27(16):5133. doi: 10.3390/molecules27165133, PMID 36014373.
36. Dabeek WM, Marra MV. Dietary quercetin and kaempferol: bioavailability and potential cardiovascular related bioactivity in humans. Nutrients. 2019;11(10):2288. doi: 10.3390/nu11102288, PMID 31557798.
37. Niu Y, Cui W, Liu R, Wang S, KE H, Lei X. Structural mechanism of SGLT1 inhibitors. Nat Commun. 2022;13(1):6440. doi: 10.1038/s41467-022-33421-7, PMID 36307403.
38. Kuswandi A, Rusdin A, Tarawan VM, Goenawan H, Lesmana R, Muchtaridi M. Molecular docking study of the major compounds from garcinia atroviridis on human sglt-2 protein transport using structure-based drug design method. Int J App Pharm. 2022;14(4):138-43. doi: 10.22159/ijap.2022v14i4.44390.
39. Himanshi Sengar C. Comparative *in silico* screening of potent peptides lead using docking strategy and ai approaches for the treatment of diabetes. J Pharm Neg Results. 2023;14:3153-64. doi: 10.47750/pnr.2023.14.03.395.
40. Arif R, Ahmad S, Mustafa G, Mahrosh HS, Ali M, Tahir Ul, Qamar M. Molecular docking and simulation studies of antidiabetic agents devised from hypoglycemic polypeptide-P of *Momordica charantia*. Bio Med Res Int. 2021;2021:5561129. doi: 10.1155/2021/5561129, PMID 34589547.
41. Pandey P, Rane JS, Chatterjee A, Kumar A, Khan R, Prakash A. Targeting SARS-CoV-2 spike protein of COVID-19 with naturally occurring phytochemicals: an in silico study for drug development. J Biomol Struct Dyn. 2021;39(16):6306-16. doi: 10.1080/07391102.2020.1796811, PMID 32698689.
42. Bisha I, Rodriguez A, Laio A, Magistrato A. Metadynamics simulations reveal a Na+ independent exiting path of galactose for the inward-facing conformation of vSGLT. PLOS Comput Biol. 2014;10(12):e1004017. doi: 10.1371/journal.pcbi.1004017, PMID 25522004.